Supplementary Information

c-MYC is required for germinal center selection and cyclic re-entry

David Dominguez-Sola, Gabriel D. Victora, Carol Y. Ying, Ryan T. Phan, Masumichi Saito, Michel C. Nussenzweig and Riccardo Dalla-Favera

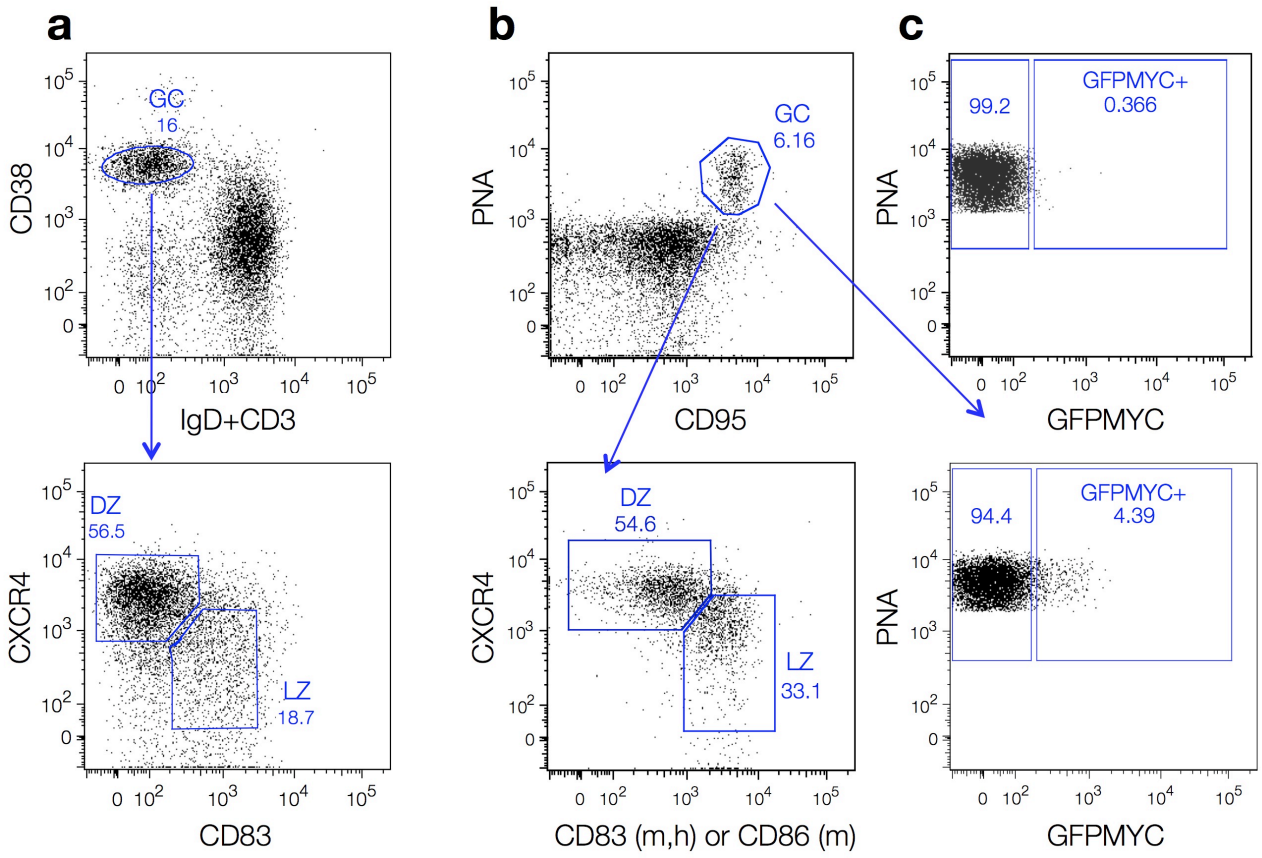

Supplementary Figure 1: Gating strategy for the identification and isolation of specific GC B cell subpopulations via Fluorescence Activated Cell Sorting (FACS). (**a**) Gating strategy to identify GC B cells (top) and LZ, DZ subpopulations (bottom) in mononuclear cell suspension from human tonsils. (**b**) Same as in (a), but applied to murine spleen and lymph node mononuclear cell suspensions. (**c**) Upon identification of GC B cells or LZ,DZ subsets in GFPMYC mice, GFP+ and GFP- cells were selected based on the gating shown in the top and bottom panels. WT mice littermates (GFPMYC-/-) were used as negative controls in order to accurately set the sorting gates (compare top and bottom panels).

Supplementary Figure 2

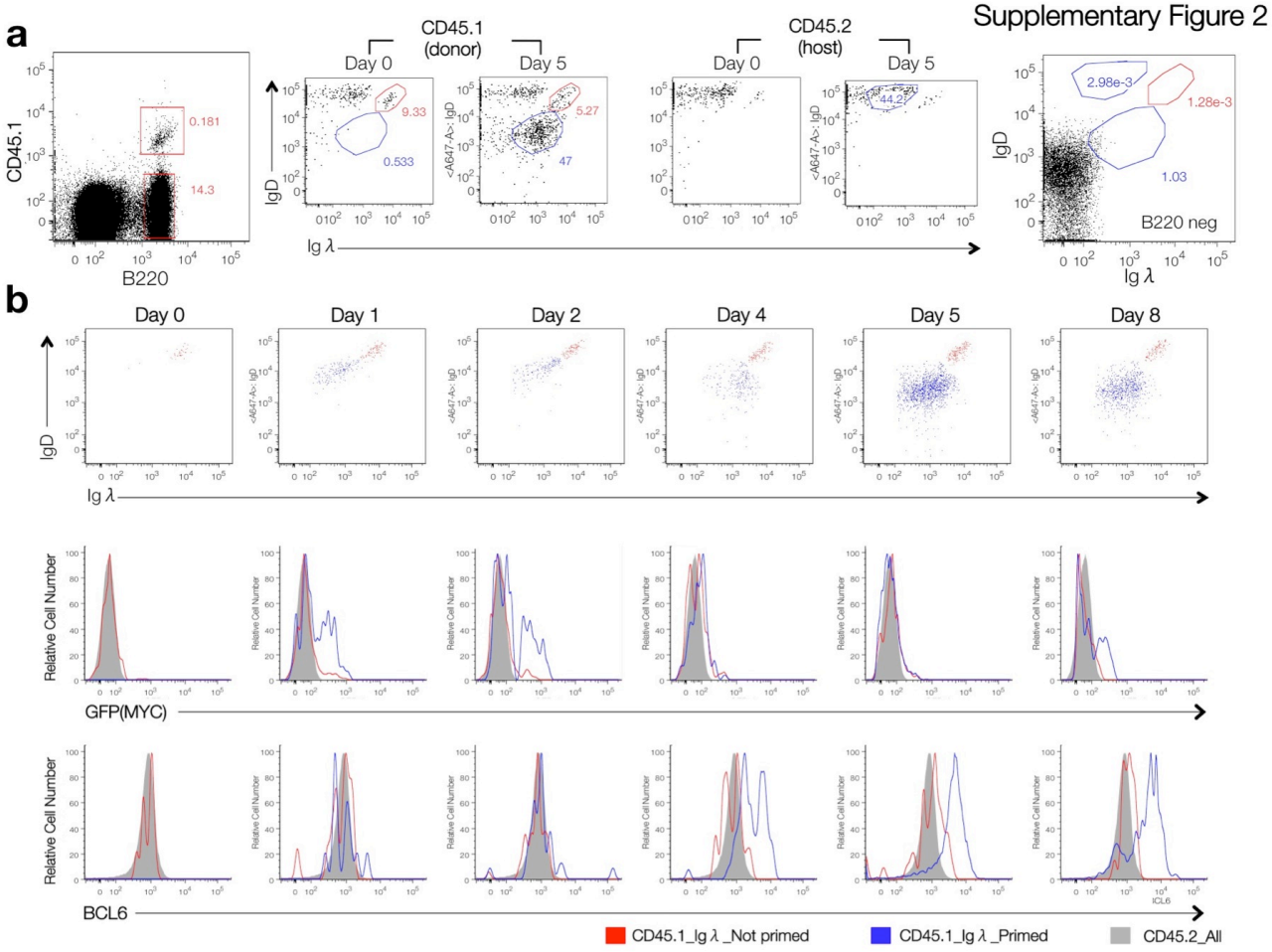

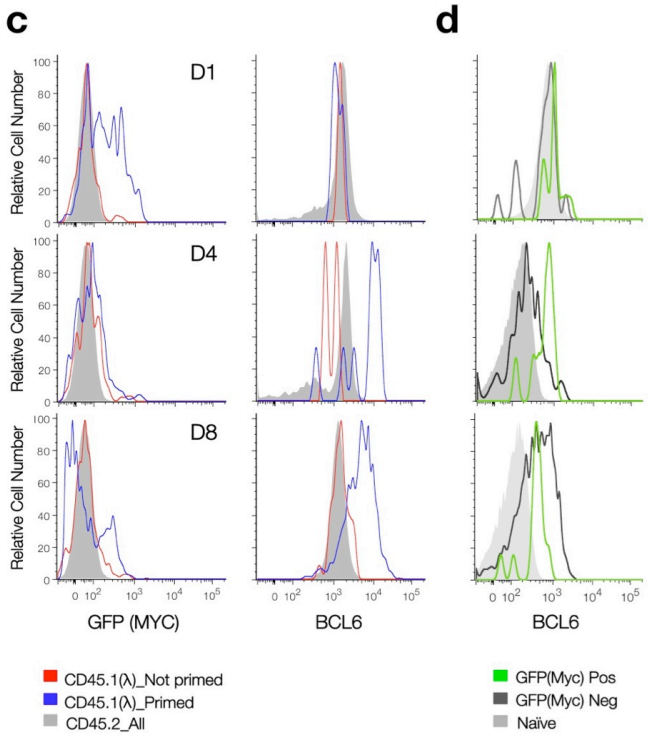

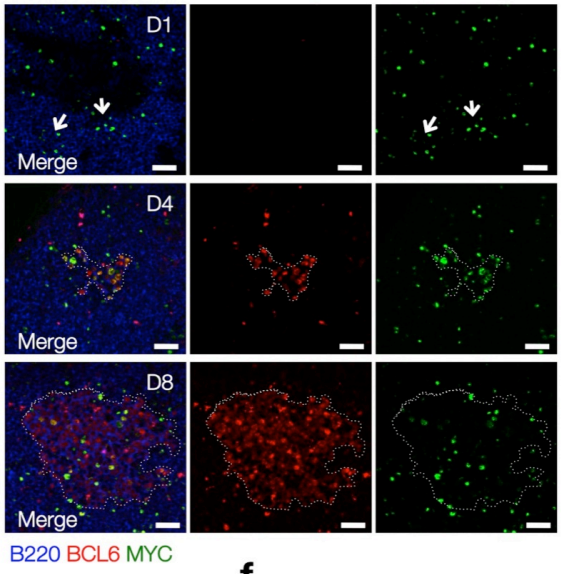

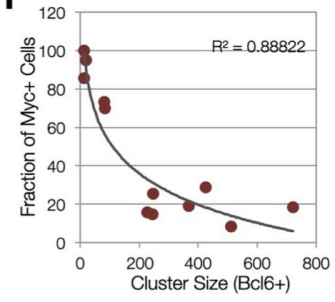

Supplementary Figure 2: Relationship between MYC and BCL6 protein expression in antigen-primed B cells and developing GC during T cell-dependent antigen responses (related to Fig.2). This is the full kinetics analysis of the experiment described in Figure 2. B1-8^{hi}/GFPMYC^{+} (CD45.1) B cells were transferred to CD45.2 host mice, and their behavior upon NP-OVA immunization followed over time. (**a**) FACS gating sequences for the analysis of each of the indicated populations. Gate coloring corresponds with the line colors in the histogram plots below (Red, CD45.1 non-primed B cells; Blue, CD45.1 primed B cells). (**b**) The **top panels** show the changes in surface expression of IgD and Igλ in antigen-primed CD45.1/Igλ B1-8^{hi} B cells. Primed cells (IgD^{hi}-Igλ^{hi} at Day 0, red cloud) internalize their B cell receptors (blue cloud, IgDλ is lost from the cell surface) and progressively expand in number, to reach a plateau between Day 5 and 8. Each dot corresponds to one FACS event. CD45.1/ Igλ B1-8^{hi} cells not primed by the antigen remain double positive (red population). **Middle and Bottom panels**: Using the same color code for each population shown in the top panels, the histograms depict the distribution of GFPMYC (middle panel) and BCL6 (bottom panel) proteins in primed and non-primed B cell populations. Shadowed grey histograms correspond to the CD45.2^{+} host B cell population, shown as negative controls. (**c**) Histograms show the distribution of GFPMYC and BCL6 expression within primed and non-primed CD45.1-Igλ B1-8^{hi} B cells (red/blue); and (**d**) the distribution of GFPMYC^{+} and GFPMYC^{-} cells (green-grey) within GC-committed (BCL6^{+}) antigen-primed B cell populations. CD45.2 host B cells, or Naïve B cells (IgD^{hi}) are used as reference. D1, D4, D8 correspond to Day 1, 4 and 8 after NP-OVA immunization, respectively. (**e**) Immunofluorescence analysis in paraffin-embedded sections corresponding to lymph nodes as in (**c,d**). Arrows in D1 highlight small clusters of MYC^{+} primed B cells. D4 and D8 show clusters of GC-committed, BCL6^{+} cells (outlined), organized within B cell follicles. Scale bars, 100 μm. (**f**) The size of BCL6^{+} clusters (cell numbers) is plotted relative to the number of MYC^{+} cells within. Measurements performed on fluorescence microscopy images of individual clusters using the "Cell Counter" plug-in in ImageJ software (Rasband, WS., ImageJ, NIH, Bethesda, Maryland, USA, http://imagej.nih.gov/ij/, 1997-2011). The linear regression curve and p-value are plotted within the image.

Supplementary Figure 3

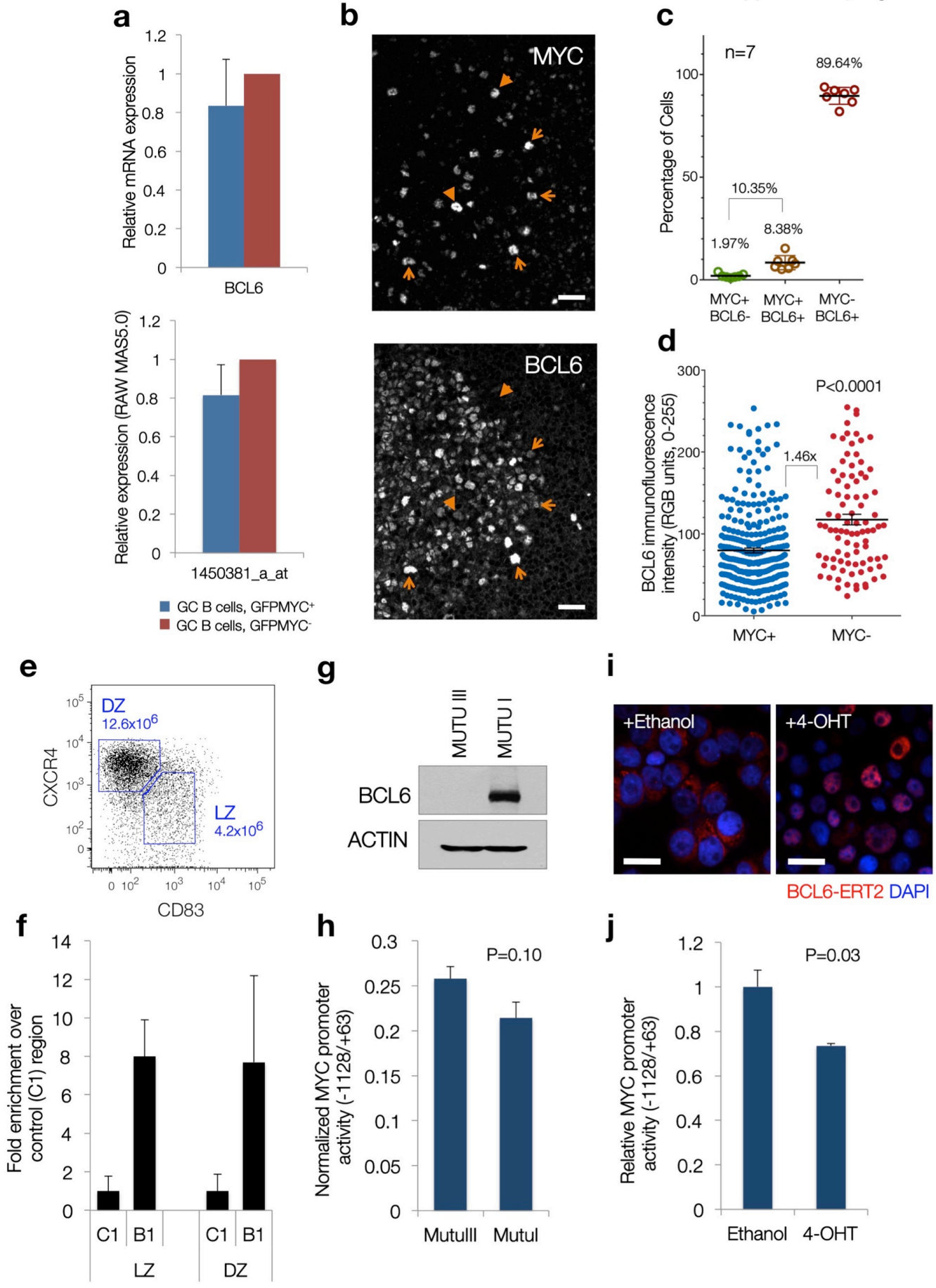

Supplementary Figure 3: Analysis of the relationship between MYC and BCL6 expression in mature germinal centers (related to Fig. 3). (**a**) Top panel, quantitative RT-PCR analysis of *Bcl6* mRNA levels in GFPMYC$^+$ and GFPMYC$^-$ GC B cells. Average of 3 mice, 3 technical replicates per mouse. Error bars, SD. Bottom panel, relative levels of *Bcl6* mRNA in GFPMYC$^+$ and GFPMYC$^-$ GC B cell samples, gene expression profile raw data in Affymetrix Mouse 430.2 genome arrays (see Methods online). Average of 4 mice per group. Error bars, SD. (**b**) Immunofluorescence analysis of MYC and BCL6 expression in a human GC (reactive lymph node). Orange arrows point to cells in which MYC and BCL6 protein co-expression is evident. Arrowheads point to cells with exclusive MYC protein expression. The bulk of GC B cells are BCL6$^+$, MYC$^-$. Scale bars, 50 μm. (**c**) GC stained as shown in panel (**b**) were analyzed by counting single cells (>5,000 cells, corresponding to 7 GCs) and the distribution of MYC and BCL6 protein expression in each cell scored. The results are summarized in the scatter plot, along with the percentage of each population (average of 5,000 cells). P-value <0.0001 (One-way ANOVA). Note that the majority of cells (>91%) have exclusive MYC or BCL6 expression. (**d**) Using the same approach shown in (**c**) we estimated the mean fluorescence intensity (MFI, RGB channel, 0-255) of MYC and BCL6 signals using Adobe Photoshop PS3 and the 'Histogram' and 'Analysis' tools. Cells with MYC MFI above 120 (MFI range 0-255) were considered MYC$^+$. All counted cells were plotted relative to their BCL6 MFI levels. The average MFI of each group is shown by horizontal bars, along with errors bars corresponding to the SD, and the relative difference (1.46 fold) between the two groups (MYC$^+$ and MYC$^-$). P-value calculated using a two-tailed T-test (unequal variances). (**e,f**) BCL6 chromatin immunoprecipitation analysis in isolated human tonsillar LZ and DZ GC B cell fractions. Panel (**e**) shows the gating strategy (CXCR4-CD83) and number of cells isolated in each fraction from a single tonsil ($2x10^8$ mononuclear cells). Panel (**f**) shows the average of 3 technical qPCR replicates. Because of the number of cells, we only assessed binding to the B1 region (as shown in **Fig. 3** in the main text), which shows the strongest binding in bulk CD77+ GC B cells. Data represented as fold enrichment of BCL6 binding in B1 vs that found in a control region (C1, >2Kb away from B1), upon normalization for the background detected in immunoprecipitates with irrelevant same-species antibody. (**g,h**) Analysis of the transcriptional activity of a luciferase reporter construct driven by the -1128/+63 MYC promoter region in MutuI and MutuIII Burkitt Lymphoma cell lines (EBV latency type I, III).

Their different EBV latency type program is associated to the presence or absence of BCL6 protein expression, as shown in (**g**). Both cell lines were transfected with 2 μg of the luciferase reporter construct, along with a Renilla reporter construct to monitor for transfection efficiency (pRL-SV40), using Lipofectamine 2000 (Life Technologies). 48 hours after transfection cells were harvested and analyzed as reported in the Methods section, online. Shown in (**h**) is the average of two independent transfections (error bars, SD). P-value was calculated using a two-tailed T-test. (**i,j**) In a similar manner, the P493-6 B lymphoblastoid cell line[1], engineered to express a BCL6-ERT2 chimera, was transfected with 2 μg of the (-1128/+63) MYC reporter construct using Lipofectamine 2000. 48hr after transfection, cells were divided in two wells and treated in parallel with either Ethanol (vehicle) or 4-hydroxy-tamoxifen (4-OHT, 400nM) for 24 hours to induce nuclear translocation of BCL6-ERT2, as confirmed in the immunofluorescence shown in panel (**i**), scale bars, 50 μm. (**j**) Cells were harvested and Luciferase activity was assessed as described. Shown is the average of two independent transfections (error bars=SD). P-value, two-tailed T-test.

Supplementary Figure 4

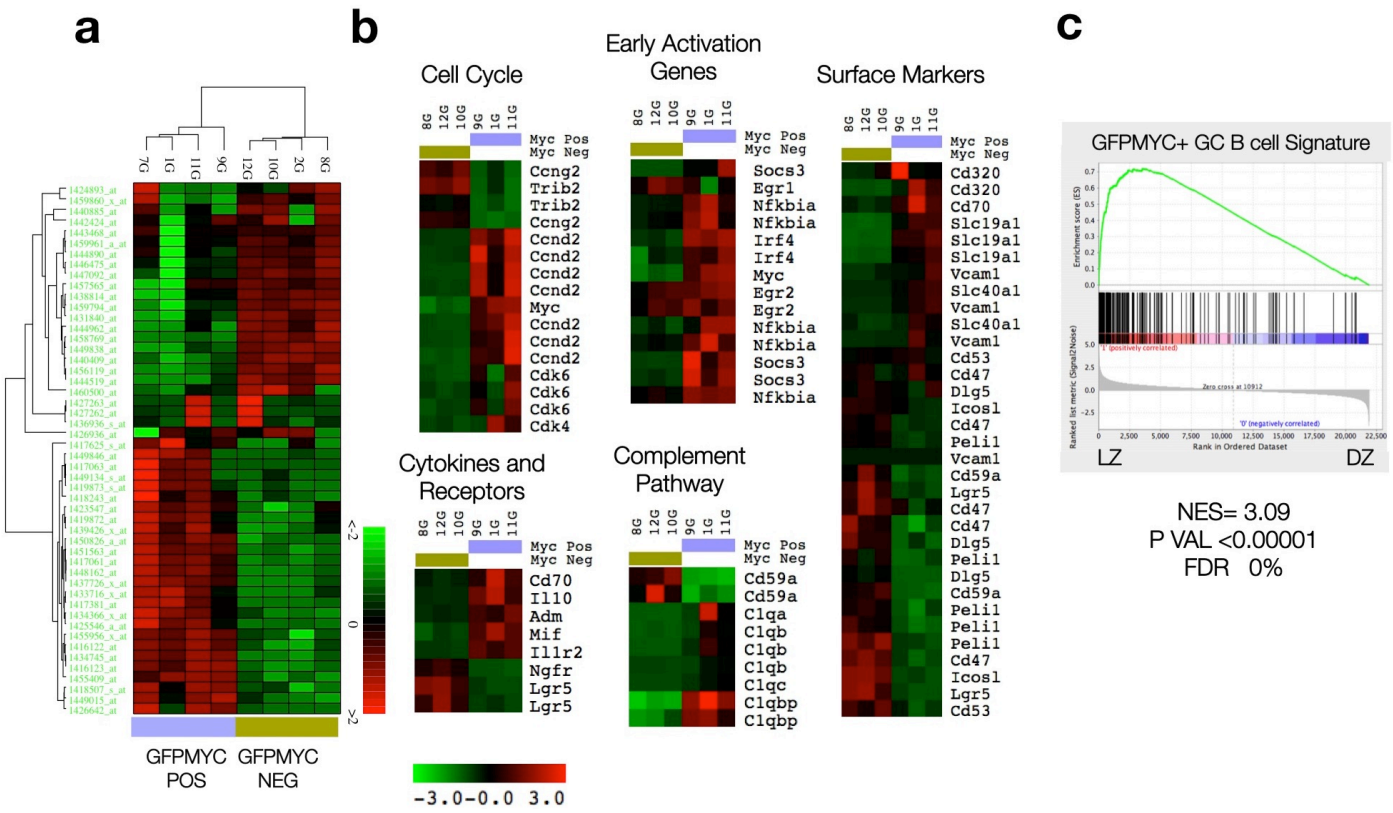

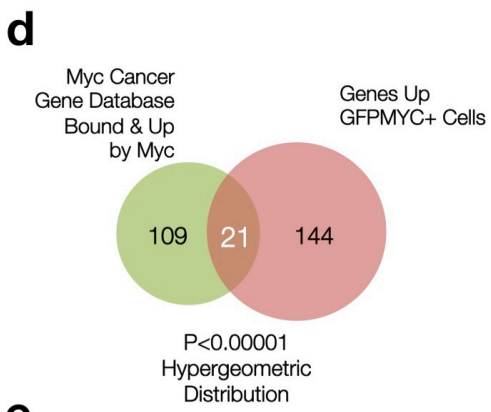

f

GENESET NAME (MSigDB)	SIZE	NES	P-VAL	FDR
SCHUHMACHER_MYC_TARGETS_UP	61	3.05	$p<1x10^{-5}$	0
DANG_MYC_TARGETS_UP	109	3.03	$p<1x10^{-5}$	0
DANG_REGULATED_BY_MYC_UP	59	2.48	$p<1x10^{-5}$	0
DANG_BOUND_BY_MYC	857	2.13	$p<1x10^{-5}$	0
BENPORATH_MYC_TARGETS_WITH_EBOX	196	2.11	$p<1x10^{-5}$	0
BENPORATH_MYC_MAX_TARGETS	634	1.89	$p<1x10^{-5}$	0
FERNANDEZ_BOUND_BY_MYC	157	1.76	$p<1x10^{-5}$	$6x10^{-4}$

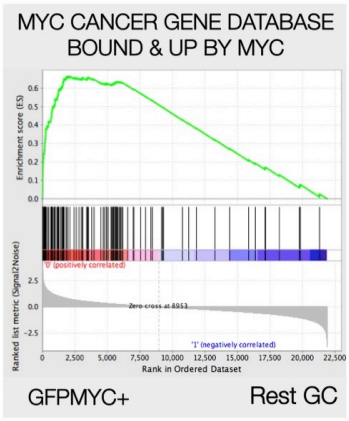

g

WANG_PRIMED T-CELL_MYC METABOLOME
SRM
SLC7A5
HK2
GLS2
LDHA
GOT2
ALDOA
CAD
GOT1
PPAT
ENO1
SLC3A2
ALDH18A1
PFKL
OAT
SMS
GFPT1
GLUD1
SLC38A1
SLC1A5
PFKFB3

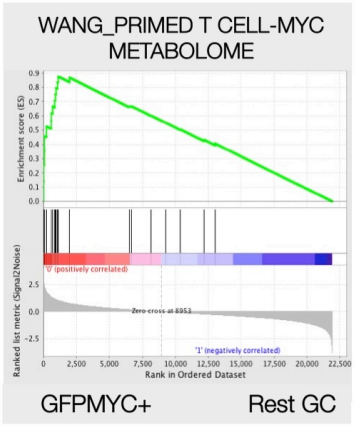

Supplementary Figure 4: Enrichment on MYC-related gene sets in GFPMYC$^+$ GC B cells (related to Table 1). (**a**) Unsupervised hierarchical clustering of gene expression data from GFPMYC$^+$ and GFPMYC$^-$ GC B cell subsets. Average linkage clustering, Euclidean metrics. Clusters were built using all genes with changes >2 fold among samples[2]. The heat map depicts the relative expression values across samples. (**b**) Summary of the results obtained after Supervised Analysis of gene expression (SPLASH algorithm; 2% delta, full support[2, 3], see Methods section online). Representative genes/probesets were distributed in GO_BP (biological process) categories, and heat maps generated using MultiExperiment Viewer (MeV v4.8; TM4 Microarray Software Suite[4]). (**c**) Gene Set Enrichment Analysis (GSEA[5]) was used to assess the distribution of the GFPMYC$^+$ gene signature across LZ and DZ GC B cell subpopulations, isolated from NP-KLH immunized mice (reported in[6]). Enrichment plot (NES, Normalized Enrichment Score; FDR, False Discovery Rate). (**d**) Venn diagram illustrating the overlap between the GFPMYC signature and a validated MYC target gene set[7] (genes physically bound and upregulated by MYC). The statistical significance was estimated using a hypergeometric distribution, considering the 6569 genes available in the Affymetrix Mouse 430.2 genome chip as the total gene population. (**e**) GSEA Enrichment plot for the previous overlap. (**f**) List of MYC-related gene signatures (Broad Institute's Molecular Signature Database, MSigDB), with significant enrichments in the gene expression profile of GFPMYC$^+$ GC B cells. Shown are signatures built in B cells, or those integrating data on chromatin immunoprecipitation data, promoter analysis and responsiveness to MYC activation. Nominal P-values and False Discovery rates (FDR) calculated using the GSEA algorithm. (**g**) Genes that integrate the "T-cell MYC metabolome" signature (metabolic genes upregulated by MYC in primed T cells, as extracted from[8]). (**h**) GSEA enrichment plot illustrating the specific enrichment for the "T-cell MYC metabolome" in GFPMYC positive GC B cells.

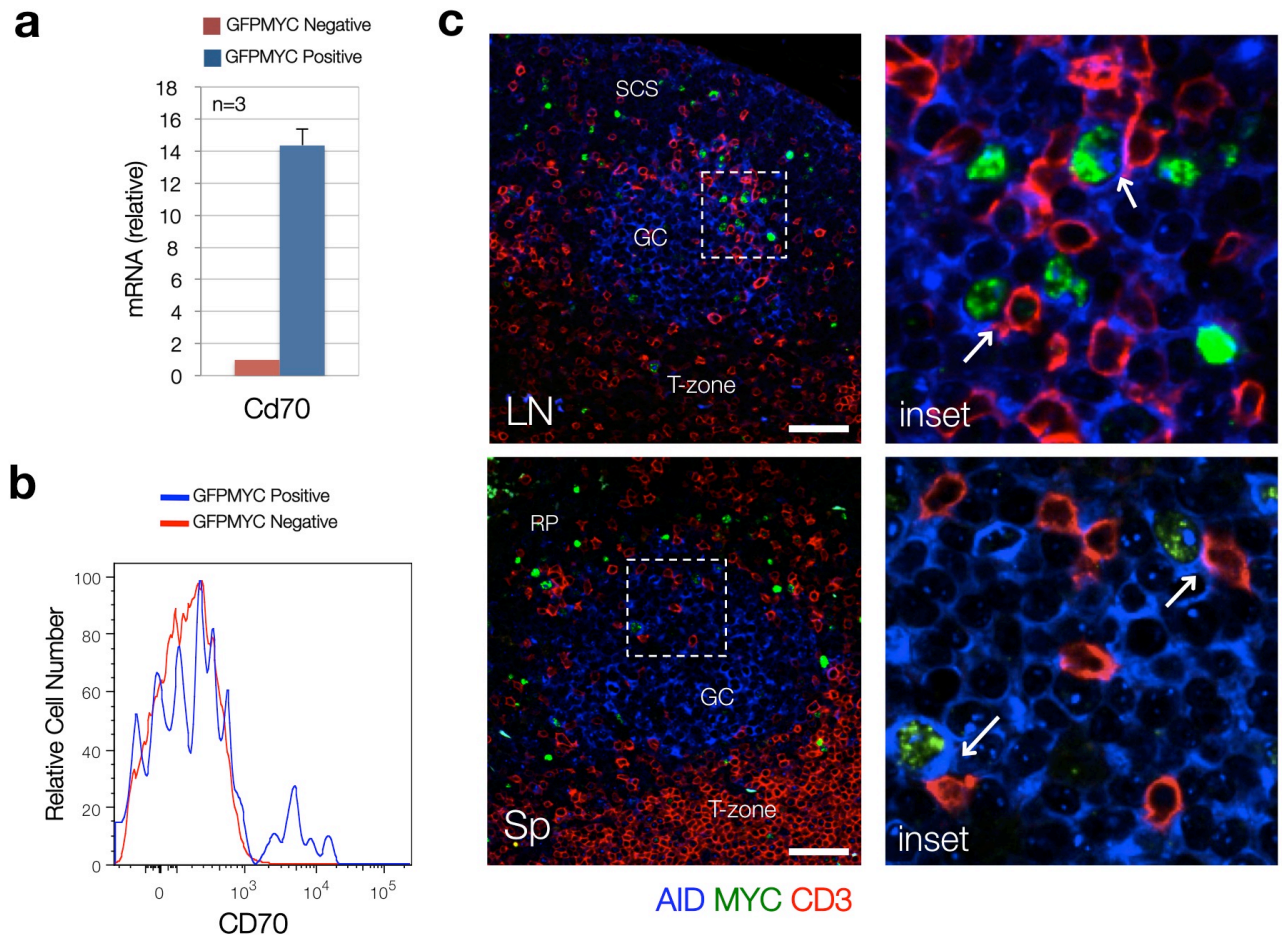

Supplementary Figure 5: MYC$^+$ GC B cells neighbor T cells and upregulate the activation marker CD70 (related to Figure 6). (**a**) Quantitative analysis of *Cd70* (*Tnfsf7*) mRNA expression in GC B cell subsets. Shown is the average of 3 independent experiments, 2 mice per experiment. Error bars=SD. (**b**) Histogram depicting the distribution of surface Cd70 protein in GC B cell subpopulations from spleens of SRBC-immunized GFPMYC$^+$ mice. Shown is a representative experiment (n=3). (**c**) Immunofluorescence on paraffin-embedded sections of lymph node (LN) and spleen (Sp) (12 days after SRBC immunization). T cells, CD3 surface staining (red); MYC$^+$ GC B cells, MYC nuclear staining (green); GC, AID staining (blue). SCS, lymph node subcapsular sinus; T-zone, T cell zone; RP, red pulp (spleen). The white arrows point to MYC$^+$ GC B cells neighbored by T cells in the LZ of GCs. Scale bar, 50 μm.

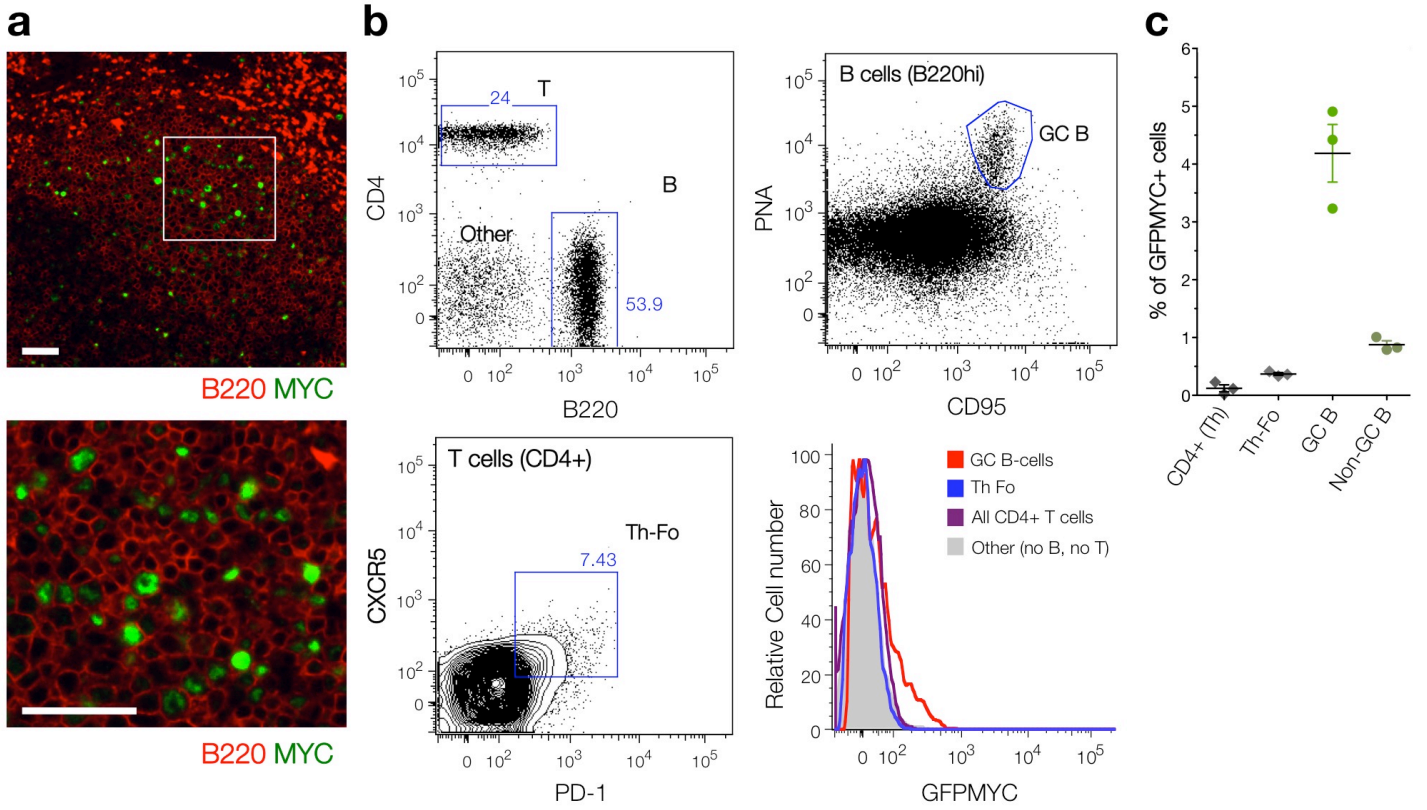

Supplementary Figure 6: MYC expression within the GC is restricted to B cells (related to Figure 7). (**a**) Immunofluorescence analysis of paraffin-embedded sections of mouse spleens, 12 days after SRBC immunization. B cells are highlighted by surface B220 (CD45R) expression (red). MYC^{+} cells are shown in green. The white square is centered on the GC, from which an inset is shown in the panel below. Note the presence of surface B220 in all MYC^{+} cells. Scale bars= 50 μm. (**b**) Dot plots show the gating strategy to define GC B cells (PNA^{hi}-$CD95^{hi}$), T-helper cells (Th, CD4+), Follicular T-helper (Th-Fo, CD4+, $CXCR5^{hi}$, $PD\text{-}1^{hi}$) and non-B non-T subpopulations in suspensions of mononuclear cells from mouse spleens, 12 days after SRBC immunization. The relative levels of GFPMYC in these three populations are shown in the histograms on the bottom right panel; and quantified in the scatter plot shown in panel (**c**). P-value of the differences between GC B cells and T cells, $p<0.0001$(One-way ANOVA; Bonferroni Multiple Comparison test correction). Note the restriction of GFP expression to B cell subsets.

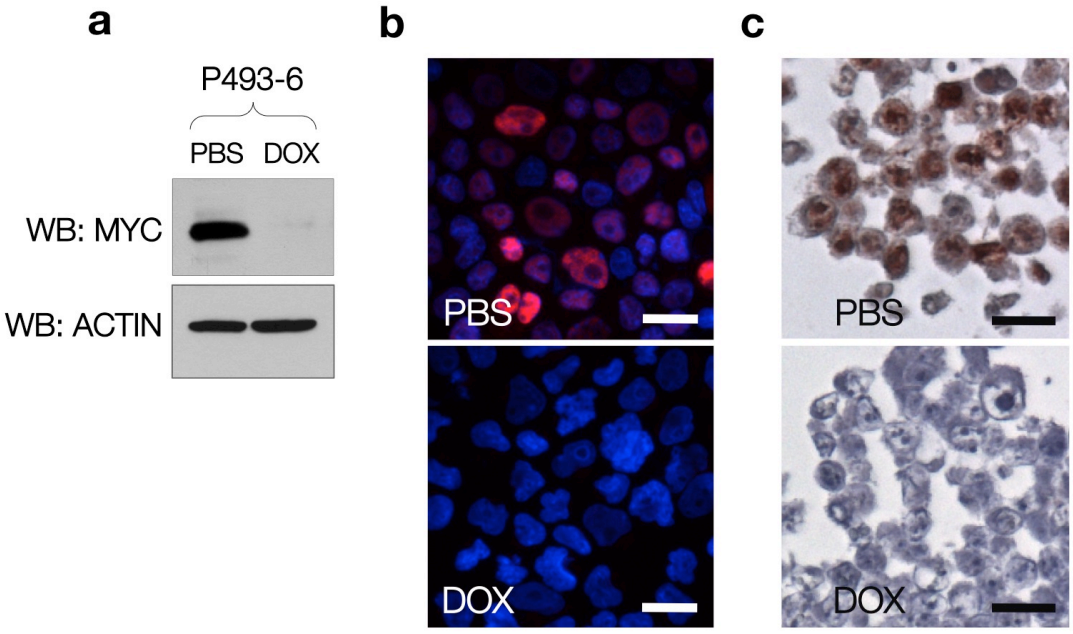

Supplementary Figure 7: Technical validation of the anti-MYC (clone Y69) rabbit monoclonal antibody (associated to the Methods online section). (**a**) Immunoblot in whole cell lysates from the lymphoblastoid cell line P493-6[1]. MYC protein expression is absent in the presence of Doxycycline in the culture medium. (**b,c**) Cells were treated with PBS or Doxycyline (1 μg/ml) for 24 hours, and harvested for immunoblot, cytospins prepared for immunofluorescence analysis (panel **b**) or formalin-fixed, paraffin-embedded cell pellets (panel **c**) prepared for immunohistochemical analysis (Scale bars, 50 μm). The strict correlation of the immunofluorescence (MYC stained in red, Cy3 dye) and immunohistochemical (MYC stained in brown, HRP-AEC) with presence or absence of MYC expression (immunoblot) confirms the specificity of the Y69 antibody.

SUPPLEMENTARY TABLES

Supplementary Table 1: BCL6 ChIP-on-chip binding profile across the proximal region of the MYC locus (NCBI36-hg18 Genome Assembly). Provided in Excel format, available online.

Supplementary Table 2: GFPMYC signature genes.

Provided in Excel format, available online.

Supplementary Table 3: Gene Set Enrichment Analysis of GFPMYC signatures (related to Table 1).

Full compendium of all results. Provided in Excel format, available online.

Supplementary Table 4: Consensus immune activation signature (related to Fig.4).

Identity of Immune Activation Signatures obtained from literature and signature databases, and full list of genes found to be present in 2 or more gene signatures related to immune activation .

GENESET NAME	Size	NES	P-val	FDR
DIRMEIER_LMP1_RESPONSE_LATE_UP	42	2.47	$<1x10^{-5}$	0
BCR_IGM_STAUDT	75	2.40	$<1x10^{-5}$	0
MARZEC_IL2_SIGNALING_UP	95	2.35	$<1x10^{-5}$	0
BASSO_CD40_SIGNALING_UP	81	1.56	$<1x10^{-5}$	0.013
GOLDRATH_ANTIGEN_RESPONSE	329	1.39	$<1x10^{-5}$	0.049
GLYNNE_FOREIGN_ANTIGEN_1H_UP	81	1.13	0.23	0.239
IL6_STAUDT	33	1.88	$<1x10^{-5}$	0.016
JAK_IL10_STAUDT	29	1.72	$<1x10^{-5}$	0.016

NES, Normalized Enrichment Score; FDR, False Discovery Rate. GSEA algorithm.

Consensus Immune Activation Signature ($p=1.27x10^{-7}$, hypergeometric distribution)

GENE SYMBOL	Gene Name (Description)
AHR	Aryl-hydrocarbon Receptor
BCL2	Predicted Gene 3655; B-cell Leukemia/Lymphoma 2
BCL2L1	Bcl2-like 1
BIRC3	Baculoviral IAP Repeat-containing 3
CCL3	Chemokine (C-C Motif) Ligand 3
CCL4	Chemokine (C-C Motif) Ligand 4
CCND2	Cyclin D2
CD70 (TNFSF7)	CD70 Molecule
CD83	CD83 Antigen
CFLAR	CASP8 And FADD-like Apoptosis Regulator
DUSP2	Dual Specificity Phosphatase 2
EGR1	Early Growth Response 1
EGR2	Early Growth Response 2
ELL2	Elongation Factor RNA Polymerase II 2
GADD45B	Growth Arrest and DNA-damage-inducible 45 Beta

GARS	Glycyl-tRNA Synthetase
GART	Phosphoribosylglycinamide Formyltransferase
HK2	Hexokinase 2
IER3	Immediate Early Response 3
IL10	Interleukin 10
IL1R2	Interleukin 1 Receptor, Type II
IRF4	Interferon Regulatory Factor 4
JUND	Jun Proto-oncogene Related Gene D
MAPKAPK2	MAP Kinase-activated Protein Kinase 2
MEF2C	Myocyte Enhancer Factor 2C
MIF	Macrophage Migration Inhibitory Factor-like
MYC	Myelocytomatosis Oncogene
PIM1	Proviral Integration Site 1
PPP1R15A	Protein Phosphatase 1, Regulatory (Inhibitor) Subunit 15A;
RGS1	Regulator of G-protein Signaling 1
SERPINB9	Serine (Or Cysteine) Peptidase Inhibitor, Clade B, Member 9
SLC3A2	Solute Carrier Family 3 (Activators Of Dibasic And Neutral
SPP1	Secreted Phosphoprotein 1
TNFAIP8	Tumor Necrosis Factor, Alpha-induced Protein 8
TNFRSF12A	Tumor Necrosis Factor Receptor Superfamily, Member 12a
TNFRSF1B	Tumor Necrosis Factor Receptor Superfamily, Member 1b
UCK2	Uridine-cytidine Kinase 2
ZFP36	Zinc Finger Protein 36

Supplementary Table 5: Summary of sequencing results on VH186.2-JH2 segments of GC B-cells (LZ MYC+, LZ MYC- and DZ), after NP-KLH immunization (related to Figure 5).

All sequences were aligned to germline Vh186.2 and JH2 segments, using the IMGT- V Quest tool (www.imgt.org). The summary of two independent experiments is shown.

	LZ, GFPMYC+		**LZ, GFPMYC-**		**DZ, GFPMYC-**	
W33L (CDR1) (W33L/Total mut) (%Exp1-%Exp2)	22% (19/86) (29%-14%)		1.1% (1/88) (2%-0%)		5.4% (5/92) (8.8%/2%)	
R/S ratio (V) (Exp1/Exp2) (Non silent/Silent)	5.575 (5.96/4.85) (201/40)		3.21 (4.09/2.20) (199/62)		2.58 (2.49/2.75) (194/75)	
	CDR	*FR*	*CDR*	*FR*	*CDR*	*FR*
R/S ratio, CDR/FR (Non silent/silent)	21 (105/5)	2.74 (96/35)	4.62 (74/16)	2.71 (125/46)	2.85 (80/28)	2.42 (114/47)
Ts/Tv (Exp1/Exp2) (Total Ts/Total Tv)	1.55 (2.35/0.67) (160/103)		1.40 (1.12/2.17) (152/108)		1.35 (1.47/1.18) (154/114)	
D segment[#] (Exp1/Exp2)	DFL16.1=95% (100/90)		DFL16.1=84.7% (81/88)		DFL16.1=79% (78/80)	

Replacement/silent ratios (R/S) are calculated for the whole V segment, and shown below for each CDR/FR regions. [Ts, transitions); Tv, transversions]. [#] DFL16.1 segments are preferentially used in BCR with high affinity for NP[9-11].

Supplementary Table 6: List of primers used in real-time quantitative RT-PCR (qRT-PCR), quantitative chromatin immunoprecipitation (qChIP) and IgH-V gene sequence analysis.

BED format file, available online.

Supplementary Table 7: Antibodies used for Flow Cytometry (FC), Immunofluorescence analysis on paraffin-embedded tissues (IF), Western Blot (WB) and Chromatin Immunoprecipitation (ChIP).

Molecule/Antigen	Application	Species	Fluorochrome	Clone	Manufacturer
B220	FC	Mouse	PCP	RA3-6B2	BD
B220	FC	Mouse	A450	RA3-6B2	eBioscience
CD4	FC	Mouse	APC	RM4-5	BD
PNA	FC	Mouse	Biotin	FL-1071	Vector
PNA	FC	Mouse	FITC	FL-1071	Vector
CD95 (FAS)	FC	Mouse	PE	Jo2	BD
CD95 (FAS)	FC	Mouse	PE-Cy7	Jo2	BD
CD38	FC	Mouse	A700	90	BD
CD70	FC	Mouse	PCP-eFluor710	FR70	eBioscience
CD86	FC	Mouse	APC	GL1	eBioscience
CXCR4	FC	Mouse	PCP-eFluor710	2B11	eBioscience
CXCR4	FC	Mouse	PE	2B11	eBioscience
CD45.1	FC	Mouse	PCP Cy5.5	A20	BD
CXCR5	FC	Mouse	PE	SPRCL5	eBioscience
PD-1 (CD279)	FC	Mouse	Biotin	RMP1-30	Biolegend
BCL6	FC	Mouse	PE	K112-91	BD
IgD	FC	Mouse	A647	11.26c.2a	Biolegend
Igλ$_{1-3}$	FC	Mouse	A700	R26-46	BD
Igκ	FC	Mouse	Biotin	187.1	BD
CD38	FC	Human	PE	HIT2	BD
IgD	FC	Human	FITC	IA6-2	BD
CD3	FC	Human	FITC	UCHT1	BD
CXCR4	FC	Human	PE-Cy7	12G5	BioLegend
CD83	FC	Human	Biotin	HB15e	BioLegend
Streptavidin	FC	-	APC		BD
Streptavidin	FC	-	eFluor450		eBioscience

Supplementary Table 7, continued.

Molecule/Antigen	Application	Specificity	Conjugate	Clone	Manufacturer
CD23	IF	Human	-	NCL-23 (mouse)	Novocastra
MYC	IF	Human/Mouse	-	Y-69 (rabbit)	Epitomics
MYC	WB	Human/Mouse	-	9E10+C33 (mouse)	Santa Cruz Biotechnology
BCL6	IF	Human/Mouse	-	GI191E/A8 (mouse)	Cell Marque
BCL6	FC/IF	Human/Mouse	PE / none	K112-91 (mouse)	BD
BCL6	WB	Human/Mouse	-	#4242 (rabbit)	Cell Signaling
BCL6	ChIP	Human/Mouse	-	N3 (sc-858)	Santa Crux Biotechnology
Beta-ACTIN	WB	Human/Mouse	-	AC-74	Sigma
AID	IF	Human/Mouse	-	MAID-2 (rat)	eBiosciences
CD3ε	IF	Human/Mouse	-	M-20 (sc-1127) (goat)	Santa Cruz Biotechnology
IgG (H+L)	IF	Mouse	-	Cat #1010-01	Southern Biotech
PNA	IF/FC	Mouse	Biotin	FL-1071	Vector
GFP	IF	-	A555	Cat #A31851	Life Technologies

Secondary Antibodies

Anti-Rabbit	IF		EnVision+ System Labelled Polymer HRP	Cat #K4002	Dako
Anti-Mouse IgG1	IF		Biotin	A85-1	BD
Anti-Rat	IF		Biotin	Cat # 6430-08	Southern Biotech
Anti-Goat	IF		Cy3	Cat # 705-105-003	Jackson Immunoresearch
Streptavidin-Cy3	IF		Cy3	Cat # 016-160-084	Jackson Immunoresearch
Neutravidin-A350	IF		A350/AMCA	Cat # A11236	Life Technologies/Molecular Probes

REFERENCES

1. Schuhmacher, M. *et al.* Control of cell growth by c-Myc in the absence of cell division. *Curr Biol* **9**, 1255-1258 (1999).

2. Klein, U. *et al.* Gene expression profiling of B cell chronic lymphocytic leukemia reveals a homogeneous phenotype related to memory B cells. *J Exp Med* **194**, 1625-1638 (2001).

3. Califano, A., Stolovitzky, G. & Tu, Y. Analysis of gene expression microarrays for phenotype classification. *Proceedings / ... International Conference on Intelligent Systems for Molecular Biology ; ISMB. International Conference on Intelligent Systems for Molecular Biology* **8**, 75-85 (2000).

4. Saeed, A.I. *et al.* TM4: a free, open-source system for microarray data management and analysis. *BioTechniques* **34**, 374-378 (2003).

5. Subramanian, A. *et al.* Gene set enrichment analysis: a knowledge-based approach for interpreting genome-wide expression profiles. *Proc Natl Acad Sci U S A* **102**, 15545-15550 (2005).

6. Victora, G.D. *et al.* Identification of human germinal center light and dark zone cells and their relationship to human B cell lymphomas. *Blood* (2012).

7. Zeller, K.I., Jegga, A.G., Aronow, B.J., O'Donnell, K.A. & Dang, C.V. An integrated database of genes responsive to the Myc oncogenic transcription factor: identification of direct genomic targets. *Genome biology* **4**, R69 (2003).

8. Wang, R. *et al.* The transcription factor Myc controls metabolic reprogramming upon T lymphocyte activation. *Immunity* **35**, 871-882 (2011).

9. Shih, T.A., Meffre, E., Roederer, M. & Nussenzweig, M.C. Role of BCR affinity in T cell dependent antibody responses in vivo. *Nat Immunol* **3**, 570-575 (2002).

10. Shih, T.A., Roederer, M. & Nussenzweig, M.C. Role of antigen receptor affinity in T cell-independent antibody responses in vivo. *Nat Immunol* **3**, 399-406 (2002).

11. Rajewsky, K., Forster, I. & Cumano, A. Evolutionary and somatic selection of the antibody repertoire in the mouse. *Science* **238**, 1088-1094 (1987).